Hybrid Electricity and Health: Effects of Renewable Energy Integration on Respiratory Illness

Austin J. Cappon

ABSTRACT

1.6 billion individuals do not have access to electricity. An additional 1 billion do not have access to electricity in a dependable form, and are often reliant on diesel generators to provide intermittent energy. Combustion of diesel is inefficient, environmentally degradative, and expensive. More harmful yet is the particulate matter (PM) released in the process of diesel combustion, which contains a class of compounds with known adverse human health effects, including cancers and chronic respiratory illnesses. In this study I modeled PM exposure rates of individuals living in a rural village on the Galápagos Islands who rely on diesel for electricity provision. The results demonstrate the capabilities of renewable energy generation technologies as a means to offset the harmful effects of a diesel-only system. I modeled three "energy scenarios," offering 20%, 50% and 80% renewables into the grid, and compared each to an all-diesel control. The model showed appreciable decreases in gross generator emissions of particulate matter for each of the scenarios (17% decrease, 45% decrease and 62% decrease from control), although the number of exposed individuals did not decrease proportionately as a result of the prevailing weather patterns at the study site (2%, 12% and 28% decrease from control). The results demonstrate that the exposure of individuals to harmful combustion toxicants is contingent not only upon the amount and type of energy generation assets in a system, but also meteorological climate and city plan.

KEYWORDS

particulate matter (PM), pollution exposure modeling, microgrid, HOMER, ArcMap

INTRODUCTION

Provision of electricity to rural regions throughout the globe is a major promoter of poverty alleviation (Kamalapur and Udaykumar 2011). Often, provision of electric services, termed electrification, is unfeasible in these rural regions via major grid connectivity. Consequently, microgrid systems that utilize distributed generation (DG) throughout the service area, are primarily used to deliver power to customers (Prasai et al. 2010, Che and Chen 2012). These generation systems are different from major-grid networks that constitute the conventional distribution method, which are characterized by large power plants, removed from the point of consumption. DG systems incorporating diesel are a major public health concern as generators are often close in proximity to community inhabitants (Bae et al. 2008).

While reliance on diesel fueled generators for energy production in microgrids throughout the developing world has a variety of associated issues, among the most important are the direct impacts of combustion emissions on human health. Epidemiological risks are well established due to the prevalence of diesel systems in the developed world (Hesterberg et al. 2005). The toxicity of diesel emissions is well described in the literature, with emitted particle size and chemical characteristics cited as the primary problematic features (Gamble et al. 2012, Syndom et al. 2001). Exposure to these emission components is directly linked to both carcinomas and a variety of respiratory illnesses (Gamble et al. 2012, Syndom et al. 2012). Though some previous studies have championed various means of mitigating the toxic content of diesel emissions, the most effective manner of reducing risk to human health is simply through reduction of combustion (Nelson et al. 2008).

To reduce the emissions from diesel generators in microgrids, inclusion of an alternate form of energy is the only viable option if grid consumption is to remain constant throughout the serviced community. In these hybrid power systems (HPS), alternative energy most often takes the form of either wind or solar coupled with a storage medium to account for system variability (Dekker et al. 2012). In such a system, a renewable energy generator is wired into the microgrid where it can power consumer loads in real-time, or alternatively charge a system storage device if energy supply exceeds demand. When demand again exceeds renewable energy supply, stored energy can be released back into the system to minimize reliance on diesel generation (Pasai et al. 2010). Mohod and Aware demonstrated this method to be a means to drastically reduce reliance on traditional diesel generation and emissions resulting from diesel combustion (2012). The benefits of HPS include direct reduction in reliance on diesel generation by means of assuming the load in real-time, and allowing diesel generators to charge system energy storage when real time load lolls in a process known as “power cycling.” This charging system allows generators to operate closer to nameplate capacity and consequently increase thermodynamic efficiencies (Niknam et al. 2012). To date, there is little data available describing how inclusion of HPS in microgrids quantitatively reduces diesel emissions and expected incidence of respiratory related illness amongst community inhabitants.

Objectives & hypotheses

In this study I will quantify the difference in expected incidence of respiratory related illnesses in four different HPS system configurations in the small island village of Puerto Villamil in the Galápagos Islands of Ecuador. I will design four system configurations to demonstrate the effects of including varying amounts of renewables into the village’s electricity grid. Each of the scenarios will represent a progressive increase in the amount of renewables included in the system with the intention of establishing a causal relationship between amount of renewables included and emission rate of particulate matter within the system. Emission profiles, detailing exhaust toxin composition and concentration parameters from each of the generators, will be modeled for each system configuration using National Renewable Energy Lab’s (NREL) Hybrid Optimization Model for Electric Renewables (HOMER) software. Emission profiles will then be utilized to generate geographic dispersion profiles for the point sources using the National Oceanic and Atmospheric Administration’s (NOAA), Aerial Locations of Hazardous Atmospheres (ALOHA) software. Finally, these dispersion plumes will be overlaid on a census dataset in the geospatial modeling software, ArcMap, to quantify the number of individuals exposed to pollutant concentrations in excess of the EPA defined threshold limitation values (TLV), above which concentrations are theorized to have adverse respiratory effects in humans. Upon completion of my research, I anticipate there will be a strong correlation between the introduction of HPS systems and the expected decrease in incidence of respiratory related illness. The reduction in illness will likely be greatest between the control and the scenario that slightly reduces diesel generation.

METHODS

Study site

I studied the rural fishing village of Puerto Villamil located in the Galápagos Islands of Ecuador (Figure 1). The site lies more than 600 miles removed from conventional centralized electricity provision systems and thus relies solely on distributed generation in the form of diesel generators to deliver electricity to the village's approximately 2,100 inhabitants. The village is approximately 1 square kilometer and over eighty percent of the village is constructed within 500 meters of the ocean. The coordinates, in decimal degrees, for the site are
S-0.054522, E-90.964158.

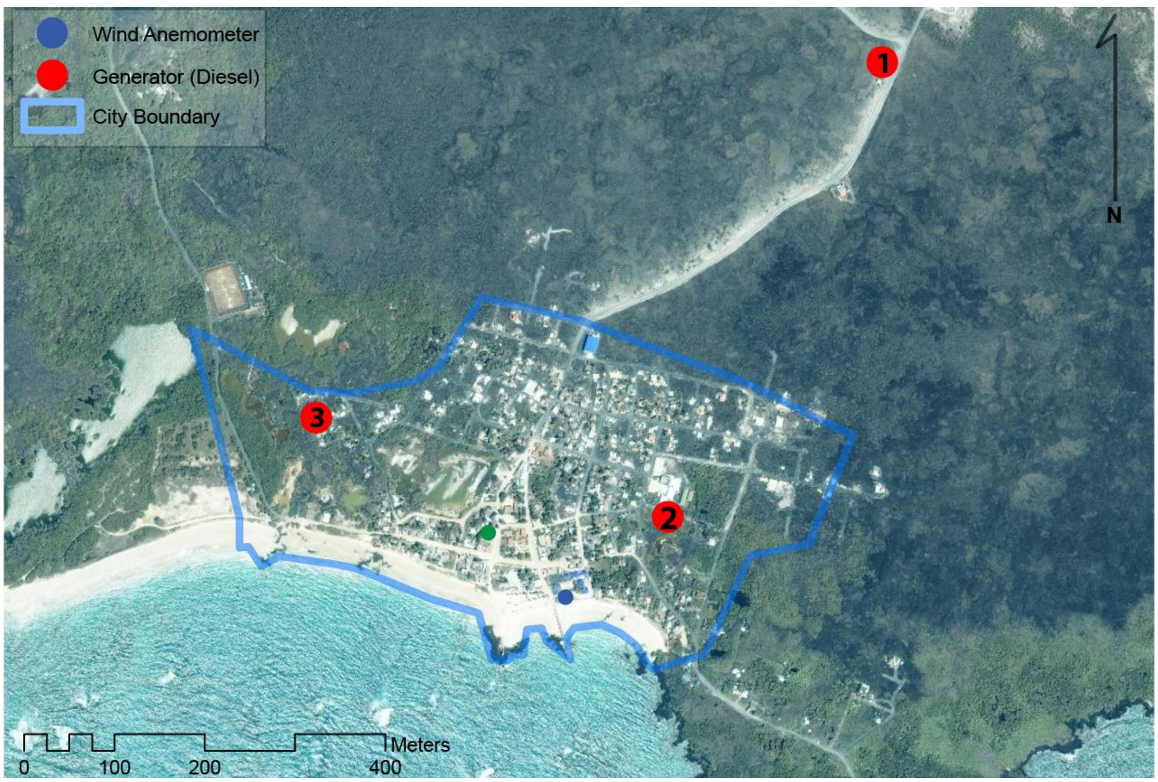

Fig. 1. Puerto Villamil Site Image. System components including existing diesel generators, and wind velocity detection location are indicated in the image.

Data collection

I gathered data from various databases and academic resource centers. Data collected included village electricity consumption parameters, village census data, orthoimagery of the island and weather observations.

I. I collected Puerto Villamil wind velocity data from the NOAA National Climatic Data Center (NCDC) for the calendar year of 2009 that provided hourly wind measurements in units of meters per second. I used the Puerto Villamil Marina weather station, located approximately 200 meters south of city center. From this data I generated monthly averages for input into HOMER (Table 1).

II. I gathered Puerto Villamil census data from the Instituto Nacional de Estadistica y Census (INEC) Ecuadorian government website (2010). The website delivered data at the resolution of a citywide census block.

III. I received Puerto Villamil electricity consumption data and current diesel generator coordinates from Elecgalapagos S.A. utility company (2011). The utility company delivered data for the month of October 2010 (Table 1).

IV. I collected orthoimagery for Puerto Villamil from Google Earth (2010).

Table 1. Data source information for Wind Velocity and Electricity consumption. Parameters represented are wind velocity and electricity consumption.

Data Type	Data Source	Data Interval	Average Data
Wind Velocity	NOAA National Climatic Data Center	Annual (2009)	10 mph 156 Degrees
Electricity Consumption	Electrogalapago S.A. utility company	Monthly (October 2010)	2720 kWh-day

I created four hypothetical scenarios representing gradual increases in total renewable energy capacity. The baseline scenario excluded renewable capacity, and served as a control. The three other scenarios included renewable energy at 20%, 50% and 80% of total generation composition (Table 2). The 20% scenario is representative of the average percentage of a renewable installation in a grid of this size (Molina et al. 2012), the 50% value is representative of a robust renewable installation, and the 80% scenario is representative of a scenario in which the grid runs entirely on renewables sources for a major portion of the year, but requires diesel generators to mitigate intermittency in renewable supply.

Table 2. Grid Specifications. Description of the electricity grid specifications for each of the 4 scenarios analyzed in the HOMER optimization model.

Scenario #	%Renew. Energy	Total Wind Turbine Capacity	Total Storage Capacity	Total Capacity of Diesel Generators	Total Village Consumption
1	0	0 kW	0 kWh	150 kW	2720 kWh/day
2	20%	60 kW	80 kWh	150 kW	2720 kWh/day
3	50%	175 kW	190 kWh	100 kW	2720 kWh/day
4	80%	3500 kW	760 kWh	40 kW	2720 kWh/day

Using HOMER, I modeled grid specifications including generator capacity, village consumption, and wind velocity to produce emissions profiles from each generator. The same annual wind data set for 2009 was used in each of the 4 assessments to ensure consistency across scenarios. As a secondary input to the assessment, I used the village electricity load profile. Using monthly electricity total values from Elecgalapagos S.A., I extrapolated daily load profiles for power consumption based on an electricity demand curve for a similar study done at low latitudes in a microgrid-serviced community of comparable size (2011, Casillas and Kammen 2011). Due to the consistent nature of this load profile on an inter-annual timescale, I used one week’s data for the entire annual model. Scenario-specific data inputs for the model included total number of diesel generators, total number of wind turbines, capacity of turbines, number and capacities of batter banks, whose values are represented in table 1. In order to ensure efficient diesel generator usage, I included power cycling as a feature of the model to ensure generators optimized their output by allowing excess power not consumed in real-time to be redirected to charging battery banks. HOMER produced pollution profiles for each generator in the form of kilograms of pollutant per year for each of the scenarios.

Pollution dispersion

To understand how the pollutants released from each of the generators dispersed throughout the region, I used the ALOHA ArcMap plugin that produces outputs of pollutant atmospheric concentration as a function of distance from emission source and atmospheric factors. This software generates accurate high-resolution models appropriate for modeling pollutant dispersion patterns appropriate for township-scale exposure studies (Tauseef et al. 2011). I inputted the following variables into the ALOHA model: location of generator, generator emission profile, and the atmospheric factors of turbidity, wind velocity, humidity and temperature. Using this data, the software produced outputs of pollution concentrations at 20-meter resolution in the area surrounding the point-source diesel generators. In order to prepare the data for post processing I utilized the "select by attribute" tool in ArcMap to select pollution polygons that exceeded concentrations of $1.5 \mu g/m^3$ PM, the threshold limitation value (TLV) for PM, at or above which chronic exposure is expected to contribute to an inflated risk in cancers and other respiratory illnesses (NAAQS 2012). Following the selection of these polygons, I exported the selected data to create new layers for each of the three generators representing the regions that contain PM concentrations in excess of the chronic critical value.

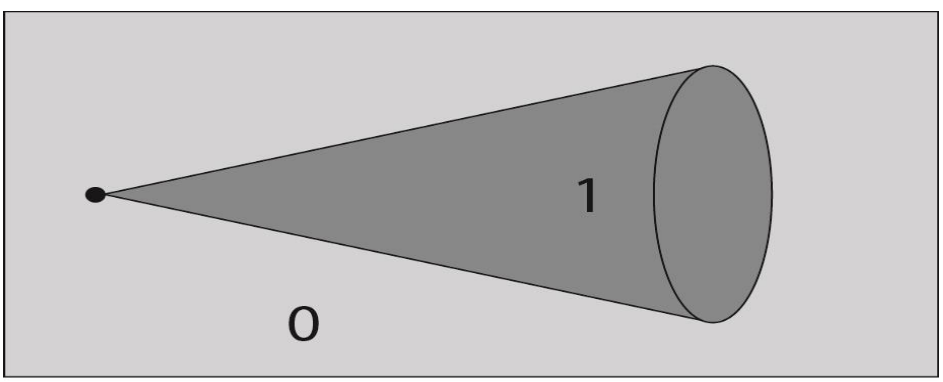

Fig. 2. Exposure classification binary scheme. In this case, "1" classifies pollutant concentrations in excess of the TLV of $1.5 \mu g/m^3$ PM. All lesser concentrations are assigned a value of "0." The logic depicted in this diagram is utilized in classification of individuals as "exposed to values in excess of TLV" or "unexposed to values in excess of TLV."

Modeling population

Using census data gathered from INEC, I extrapolated population distribution using a manual roof-count technique in ArcMap. The census data gathered from INEC existed at village scale resolution in shapefile format compatible for use in ArcMap. In order to develop population data at 20-meter resolution necessary for associating population density to air pollution concentration, I used a buffer technique to generate a 10m radius area around each rooftop point. These 10m radius circles served as a proxy for household footprints.

Pollution epidemiology

Using geospatial data layers of atmospheric pollutant concentrations and village population distributions, I modeled expected incidence of illness for each scenario by using a spatial analysis technique within ArcMap. In order to quantify the number of individuals exposed to pollutant concentrations in excess of the (TLV) of 1.5 $\mu g/m^3$, I used a spatial join technique to combine attribute tables for the residence buffer layer and the chronic threat exposure layer. Following the union of these attribute tables, I was then able to create an additional field for total population exposed in each scenario. The calculations were executed using the field calculator. I then executed the same technique for each of the four scenarios and compared the number of exposed individuals between each.

RESULTS

Generator emissions

Inclusion of renewables in the grid architecture reduced PM emissions from the diesel generators. In scenarios 2-4, the system utilized the generators for a lesser portion of total year from the baseline scenario that excluded renewable energy sources (Table 1). PM emissions decreased in a manner inversely proportional to total installed renewable capacity. Generators were cycled on in a less predictable manner between cases as a consequence of peak shaving and load cycling—processes that allow generators to charge batteries when excess power is available (Table 3, Fig. 3).

Table 3. Emission statistics for the three generators included in the model. Annual operating hours is inversely proportional to percentage of renewables included in energy mix. Power cycles vary sporadically according to grid architecture.

Scenario #	Total Annual Diesel Emissions (Kg of PM)	Combined Annual Operating Hours	Combined Power Cycles
1	435	13869	1096
2	344	11695	3763
3	255	8804	3175
4	158	6298	1608

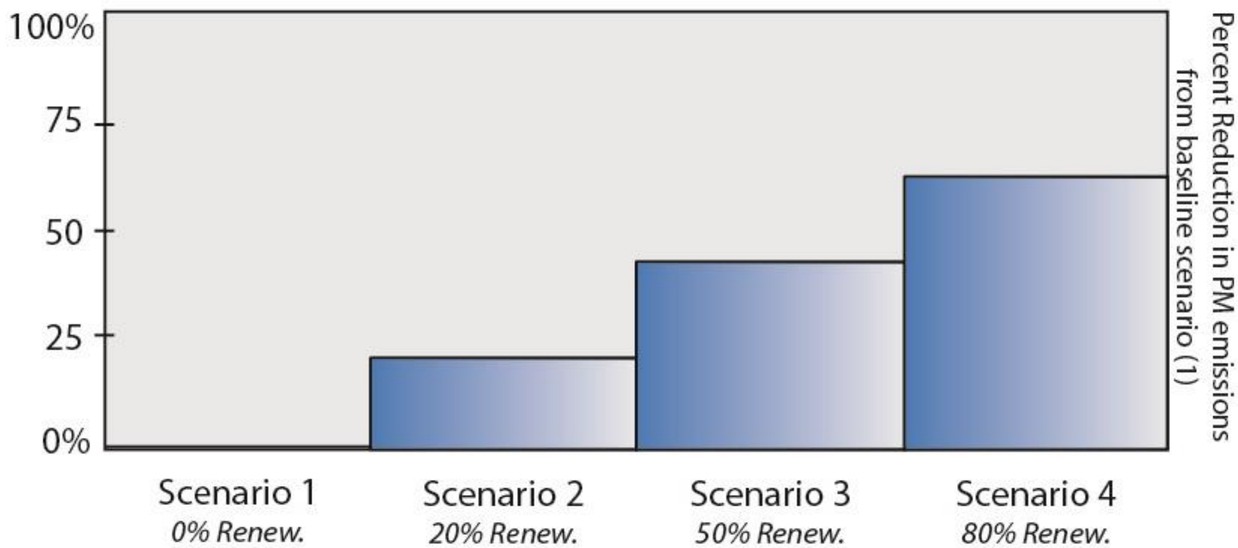

Fig. 3. Percent reduction in PM emissions for each scenario. Graph indicating percent reduction of particulate matter pollution in each of the scenarios as compared to the baseline, diesel-only scenario. Percent reduction tracked closely the percent of renewables integrated into each of the respective systems.

Pollution dispersion

Particulate matter dispersed predominantly in a northwesterly direction, with concentration as a function of distance from emission source varying only marginally with wind velocity. With wind speeds around the average of approximately 10 mph, dispersion values in excess of the TLV existed as far as 1300 m of origin. With wind speeds in excess of 14 mph detectable pollutant concentrations of 0.01 $\mu g/m^3$ dispersed as far as 10 km. The critical dispersion distance, at which the PM concentration fell to a value less than TLV, I found to be greatest in scenario 1 at 1,200 meters and least in scenario 4, at a value of 607 meters (Table 4). Greatest variance in concentrations that existed amongst sequential scenarios occurred between scenario 3 and 4 (Table 4). I found average wind speed to be 9.95 mph with a standard deviation of 5.3 mph. I found average wind direction to be 155 degrees, with a standard deviation of 50 degrees (Appendix A). Because of this relatively predictable nature of the data, I utilized ALOHA to generate critical dispersion distance values for each of the four scenarios, that represent the distance value from the generator at which particulate matter concentrations fall to a value less than 1.5 $\mu g/m^3$, the TLV (Table 4).

Table 4: Critical dispersion distances. Average annual distance at which the Particulate Matter concentration fell below the critical chronic exposure threshold of 1.5 $\mu g/m^3$, shown for each of the four scenarios.

Scenario #	1	2	3	4
Critical Dispersion Distance (m)	1200	1000	857	647

Modeling population

In order to model population, I used a rooftop count interpolation technique in conjunction with a population count for the village. Population was found to be greatest East-North-East of generator 2 (Figure 1). The rooftop count yielded a total of 233 residences. Using the population value for the whole village of 2100, I estimated average population per household to be 9 individuals. Population reached a density of 85 individuals per 100 square meters in the residential region adjacent to the generator in the southeast corner.

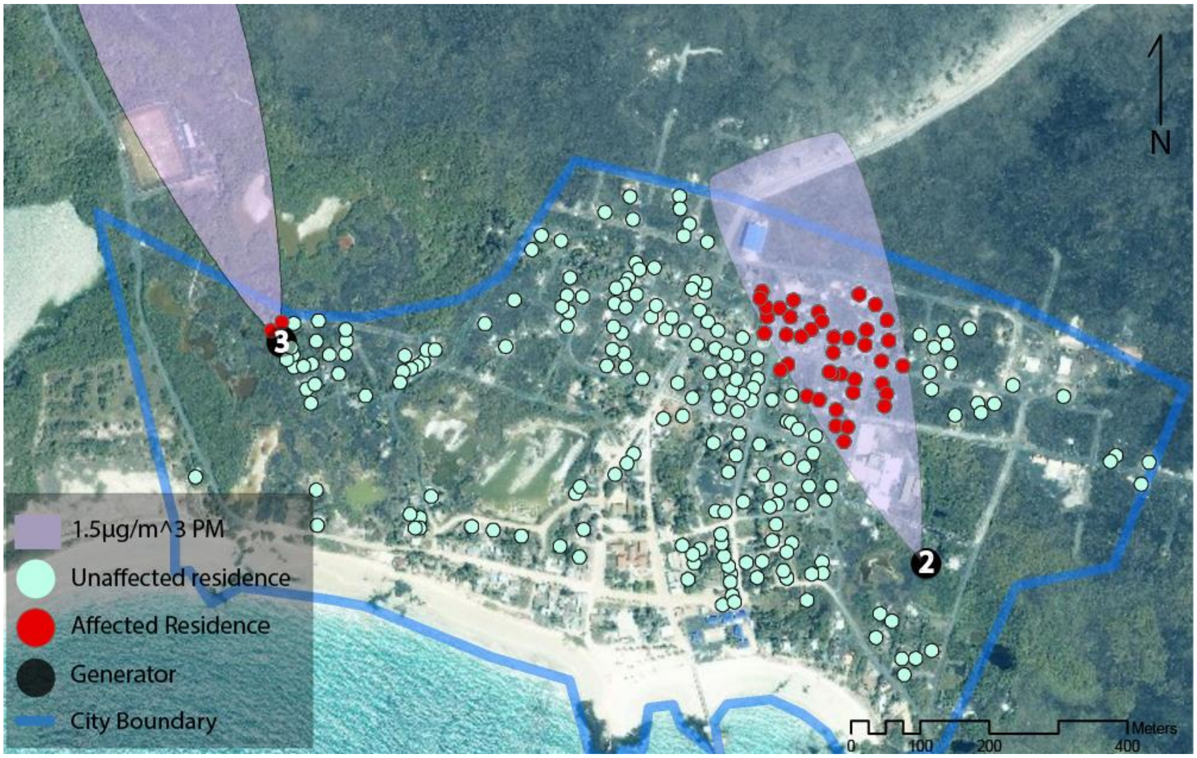

Fig. 4. Exposed individuals in scenario 1. Dispersion model for Puerto Villamil. Displayed is scenario 1, in which no renewables are included. Greatest interaction between population and pollution is evident NW of the generator 2.

Pollution epidemiology

Greatest epidemiological risk, I discovered, to exist in the baseline, diesel-only system model. The region that experienced the greatest exposure was that directly NW of generator 2 (Figure 3). 306 individuals were exposed to concentrations that met or exceed the TLV of 1.5 $\mu g/m^3$ PM in the scenario this baseline scenario. I witnessed a gradual fall off in the number of individuals exposed to toxicant concentrations in excess of TLV in scenario 2 and 3, at 297 and 270 individuals respectively (Table 5). Expectedly, the case that included 80% renewables saw the least individuals exposed to concentrations of 1.5 $\mu g/m^3$

Table 5. Exposed individuals. Number of individuals for each scenario exposed to PM concentrations greater than or equal to the Threshold Limit Value (TLV) of $1.5\,\mu g/m^3$. Greatest difference in the number of exposed individuals between sequential scenarios is seen between scenario 3 and 4.

Scenario #	**1 (0% Renew.)**	**2 (20% Renew.)**	**3 (50% Renew)**	**4 (80% Renew.)**
Individuals exposed to ≥ $\mathbf{1.5\,\mu g/m^3}$	306	297	270	216

DISCUSSION

Introduction

I found the most striking outcome of this study to be the impressive portion of the population exposed to harmful PM concentrations. More impressive still, I found to be the marginal decrease in exposure numbers despite the immense reduction in particulate matter emissions in each of the progressive HPS scenarios. The gross output of particulate matter dropped nearly 65% in scenario 4, and more than 40% in the less aggressive scenario 3 when compared to the baseline scenario. Contrastingly, the very same scenarios, resulted in a mere 28% and 11% respective reduction in individuals exposed to pollution concentrations equivalent to or greater than the TLV. The likely culprit for the disparity between the magnitude of reduction for the total PM emissions and the total exposed individuals is the invariable nature of the wind in the study system (Appendix A); throughout the course of the year, wind velocity varies only marginally, and as a consequence a very specific region is recurrently exposed to adverse concentrations of PM. Despite the relatively unexceptional reduction in exposure numbers for the scenarios, when considering the implications to the village's population, even a modest reduction is desirable.

Generator emissions

Total generator emissions for each of the three scenarios integrating renewables decreased in a semi-linear fashion. The reduction of PM emissions closely tracked the amount of integrated renewables in scenario 2, with a 20% reduction in total PM output from the baseline scenario. The reduction noted in scenario 3 equated to approximately a 41% total decrease in PM output from the scenario. Similarly the final scenario, 4, equated to a 64% reduction in total PM emissions as compared to the baseline case (Figure 2). Such a direct relationship is seen in other studies in which alternative sources of energy are integrated into an otherwise diesel-only system (Lee et al. 2013, Wijayatunga et al. 2004). For the final two scenarios, the slight difference between renewable integration and total reduction is likely due to the intermittent nature of renewables; as more renewables are integrated into a given system, the likelihood at any given point in time that all wind-dependent generation assets experience a lull in electricity output is drastically higher (Underwood et al. 2007). Though the integrated batteries help mitigate effects of intermittencies by means of energy storage, a prolonged lull in the wind would exhaust their buffering capacity, and as a consequence would require the activation of diesel generation assets. This phenomenon associated with exhausting buggering capacity of a storage medium is often witnessed in systems that incorporate an extensive proportion of renewable energy (Prodomidis and Coutelieris 2012, Yang and Walid 2013).

Dispersion

Despite the robust decrease in total emission outputs seen in each of the scenarios, I found the dispersion model to forecast marginal changes in the PM plume boundaries. While the TLV dispersion distances decreased by nearly half from scenario 1 to scenario 4, the morphology of the plumes generated changed relatively little in width. This lack of change in width resulted in relatively comparable interfaces for all scenarios between the population model and the dispersion plume. The probable cause of this stagnant width between each of the scenarios has to do with the invariable nature of the wind; the individuals most affected by the generator outputs were those in the direct wake of generator 2. The majority of the population resided in the region within about 500 meters of the generators, so these changes at the extreme ends of the plume did not result in profound decrease in the modeled exposure rate (Figure 5).

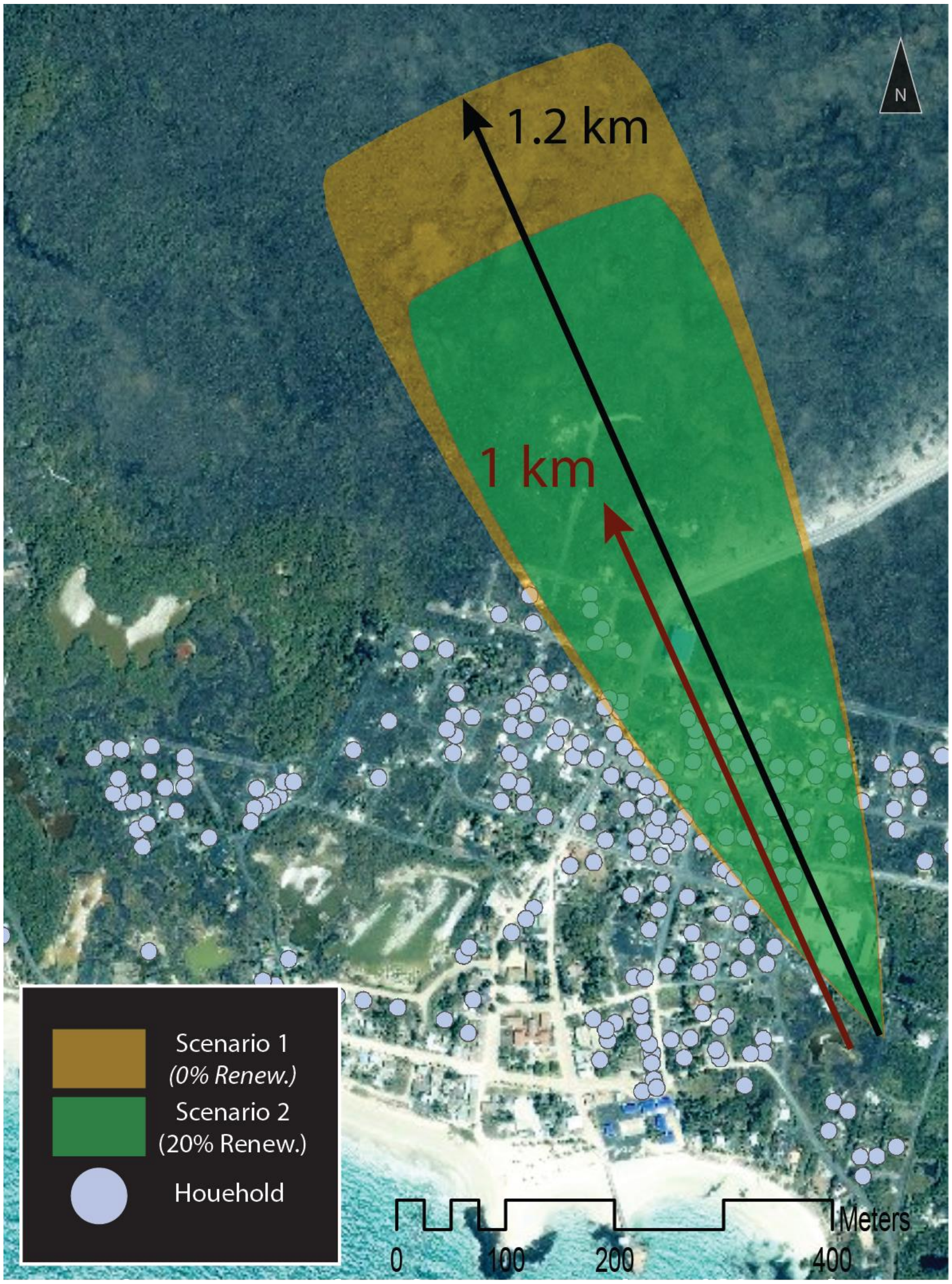

Fig. 5. **Dispersion plume morphology.** Two dispersion plumes overlaid on top of one another. The variation between the two plumes exists primarily at the extreme end of the plume, away from the population. The lateral morphology of the plume does not change much between the scenarios.

Modeling population

The rooftop count technique utilized in my study I found to be sufficient indicator of a trend of pollution exposure in the data, however for greater resolution and more statistically accurate data, geo-referenced census counts would be greatly beneficial. The rooftop count interpolation technique in conjunction with the limited census data for the region produced an average household size of 9 individuals, which is comparable to the average value for estimated for the region (INEC 2010). Despite the likely appreciable variation from this value, the estimation technique was shown in a similar study to show sufficient merit to associate forecasted population points to later empirically measured values (Wu et al. 2005). The majority of the individuals living in the region lived in the portion of the village 200 meters removed from the shore, away from the expensive tourism-centric real estate of the beachside (Figure 1).

Pollution epidemiology

Population, I observed to be, highly concentrated in the region in the direct wake of the dispersion plume of generator number 2 (Figure 4,5). The epidemiological risk to individuals, I discovered, to be proportional to the degree of renewables included in the system. I noted immense exposure values for the population sub-group residing in the downstream wake of generator 2 across all of the scenarios. The likely cause for these elevated exposure values is related to the geographic relationship between the residences and generation sources with respect to the prevailing wind direction. Generator 1 existed in such a location that its dispersion plumes rarely interfaced with the population and thereby did not contribute to the creation of any exposed individuals. Generator 3, though minimal in its contribution to the total exposure values in the site, did in fact yield 18 individuals as exposed to PM in excess of TLV. I witnessed no change in epidemiological risk for individuals living in the dispersion plumes of generator 3 across all four scenarios. The likely cause of this observation is related to the distance the population resided from the their proximal generator; the greatest changes in exposed individuals I found to exist at the plume boundaries for generator two, in the case of generator 3 the eighteen exposed individuals all resided within 50 meters of the emission source (Figure 4). As such, even shortest critical dispersion distance, which I noted to be 647 meters, drastically exceeds the physical distance between the individuals and generator 3 (Table 2).

Limitations

The most overt limitation of the study is the inherent fuzziness of the dispersion plume. Due to the mild ambiguity in this modeling technique, it seems possible for the final model to inappropriately exclude individuals living on the boundary of the dispersion plume. It is quite possible to envision a situation in which a residence lies on the arbitrary exterior boundary of a dispersion plume and, despite relentless exposure to the harmful effects represented by the plume, the household is excluded from the data set. I attempted to rectify this shortcoming by over estimating the size of the residences and thereby creating an artificial buffer around the true physical extent of the building. This artificial buffer would allow the residence to be more likely to spatially overlap with the dispersion buffer and be counted toward the total exposure values. An additional limitation of the study developed out of my population estimation technique that treated each household as identical in regards to number of resident individuals; of course there is variance in physical household size in this village as there is with any other place, and thereby a likely resulting variance of resident individuals in each of those households. Despite this shortcoming I utilized a ground-truthing technique to verify that the household physical size was at least superficially consistent, and found that such was indeed the case; with the exception of few residential households, nearly every one was single-story and occupied a seemingly standardized lot size. A final qualification for the study is embedded in the assumption that the pollution outputs are temporally fixed on an annual timescale. The dose-response curve for particulate matter exposure is not linear, and as a consequence, periodic spikes in pollution output could have acute effects on individuals within the community.

Future directions

Future investigation should focus on validating the methodology and estimation techniques utilized in this study. Perhaps the most effective technique for validating the technique would involve cross checking estimated values from the dispersion plumes to empirically measured values at the study site. This method would allow for some assurance that the estimated values are indeed what residents are experiencing. Additional efforts could also be focused on gathering more accurate population distribution data. Likely the most effective technique would be a detailed census to gather high-resolution data about the distribution of the population in the village. A final area that dictates further investigation would be a health survey to assess the observed incidence of respiratory illness as contrasted to the forecasted values.

Additional analysis

Among the most interesting findings of the study evolved out of the observed significance of generator placement relative to the population. Though not quantitatively analyzed, the variable that seemingly played the greatest role in dictating eventual exposure values, I found to be, the placement of the diesel generators relative to individuals. While both generator 2 and 3, exist in relative geographic proximity to the residential region, generator 3 contributed to a mere 18 individuals exposed to values in excess of the TLV, while generator 2 had much more drastic impacts on the population, leading to 288 exposed individuals, in the control scenario without renewables. The discrepancy in exposure for numbers between the output-identical generators is a result of the location of the generators relative to wind direction and populous regions. An alternative intervention in the electivity grid to integrating renewables, would be to simply move generator 2 to an alternate, downwind location. Such an intervention would require minimal investment and would seemingly alleviate major environmental health concerns for the population. Siting and reconfiguration of the electricity grid architecture would require professional engineers, although the costs associated with such a process would likely be much less than those for even the most modest renewable integration project.

Broader implications

The most pressing implications of this study are the forecasted adverse health effects for Puerto Villamil's population. Analysis should focus on comparing the forecasted data to empirically gathered data in the form of an on-the-ground public health study. Pending the outcome of such a study, the government of the community should interject appropriately in order to mitigate risk.

Despite the failure of renewables to appreciably mitigate the harmful effects of diesel combustion in this specific study system, I found numerous motivations for including renewables into a microgrid during my research, and would stipulate to be worthy of sufficient merit. Perhaps the most salient motivation for renewables incorporation is associated with their intrinsic reduction of reliance on conventional hydrocarbon based fuels, which are volatile in both a strictly physical sense and also in an economic sense. An additional benefit correlated with the inclusion of renewables in such a system is reduced reliance on transportation of fuel from the mainland, some 600 miles away. Carta et al. found costs of fuel transportation to an island study site to be the dominant component of the fuels price to island consumers (2003). With a reduction in reliance on this anemic link in the energy delivery chain, consumers would be liberated from enormous fuel costs imbedded within rural nature of the delivery system, and additionally better able to weather a period of prolonged isolation from fuel supply lines. Reduced reliance on imported fuel would moreover mitigate the risks associated with tanker spills in the ecologically unparalleled marine systems of the Galápagos, like those seen in the 2001 spill that resulted in catastrophic ecological damages (Edgar et al. 2003) A final aspect for motivating such a project can be associated with the direct occupational and educational benefits to the islands population who would be highly involved in the construction of the renewable infrastructure and moreover trained to tend to operation and maintenance of the generation assets and infrastructure.

Although the weather conditions on Puerto Villamil are seemingly quite unique when contrasted to a conventional, seasonally variable perception of climate, wind analysis studies demonstrate that this recurring wind pattern is common amongst many low latitude locales throughout the course of the year (Appendix C, Tomas and Webster 1997). As such, any village with similar latitude and grid composition would likely experience the same wind-determined exposure results. Due to the prevalence of diesel microgrids at low latitudes, it is quite likely that many locations throughout the globe are experiencing the very same adverse health effects as those seen in Puerto Villamil. Using only a few vital datasets from a sample site it is possible to forecast toxicant exposure leading to adverse health effects for village inhabitants. Awareness regarding potential adverse health effects is often a potent motivator for policy adaptation to promote energy reform.

ACKNOWLEDGEMENTS

I would like to acknowledge first and foremast the ES196 staff, who tirelessly committed themselves to fostering a stimulating environment for project development. Deserving of special recognition is Rachael Marzion, who read through innumerable drafts and provided insightful feedback throughout, and was always quick to lend a hand whenever the author fell short. I would also like to thank the combined efforts of Dr. Duncan Callaway and Dr. John Radke for their support in the formation of my project methodology and guidance in the often-turbulent waters of the sea of technical software. The invaluable feedback from my peer review group is too deserving of special thanks, particularly Ani Lee, for her willingness to put up with my often less-than-polished draft iterations.

REFERENCES

ALOHA: Ariel Locations of Hazardous Materials. NOAA, EPA.

ArcGIS Desktop. (2012) Environmental Systems Research Institute (ESRI).

Bae, I.-S. & Kim, J.-O. (2008) Reliability evaluation of customers in a microgrid. *Ieee Transactions on Power Systems*, **23**, 1416–1422.

Carta, J.A., Gonzalez, J. & Gomez, C. (2003) Operating results of a wind-diesel system which supplies the full energy needs of an isolated village community in the Canary Islands. *Solar Energy*, **74**, 53–63.

Casillas, C.E. & Kammen, D.M. (2011) The delivery of low-cost, low-carbon rural energy services. *Energy Policy*, **39**, 4520–4528.

Che, Y. & Chen, J. (2012) Research on Design and Control of Microgrid System. *Przeglad Elektrotechniczny*, **88**, 83–86.

Dekker, J., Nthontho, M., Chowdhury, S. & Chowdhury, S.P. (2012) Economic analysis of PV/diesel hybrid power systems in different climatic zones of South Africa. *International Journal of Electrical Power & Energy Systems*, **40**, 104–112.

Edgar, G.J., Kerrison, L., Shepherd, S.A. & Toral-Granda, M.V. (2003) Impacts of the Jessica oil spill on intertidal and shallow subtidal plants and animals. *Marine Pollution Bulletin*, **47**, 276–283.

Elecgalapagos S.A. Utility Company. (2011) Utility Company. URL http://www.elecgalapagos.com.ec/es/index.php

Gamble, J.F., Nicolich, M.J. & Boffetta, P. (2012) Lung cancer and diesel exhaust: an updated critical review of the occupational epidemiology literature. *Critical reviews in toxicology*, **42**, 549–598.

Google Earth. (2010) Google.

Hesterberg, T.W., Bunn, W.B., McClellan, R.O., Hart, G.A. & Lapin, C.A. (2005) Carcinogenicity studies of diesel engine exhausts in laboratory animals: A review of past studies and a discussion of future research needs. *Critical Reviews in Toxicology*, **35**, 379–411.

HOMERENERGY. (2010) *HOMER: Hybrid Optimization Modeling Software*. National Renewable Energy Lab.

INEC. (2010) Census, Instituto Nacional de Estadistica y Censos, Ecuador.

Kamalapur, G.D. & Udaykumar, R.Y. (2011) Rural electrification in India and feasibility of Photovoltaic Solar Home Systems. *International Journal of Electrical Power & Energy Systems*, **33**, 594–599.

Lee, K.-J., Shin, D., Yoo, D.-W., Choi, H.-K. & Kim, H.-J. (2013) Hybrid photovoltaic/diesel green ship operating in standalone and grid-connected mode - Experimental investigation. *Energy*, **49**, 475–483.

Liu, W.T., Tang, W. & Xie, X. (2008) Wind power distribution over the ocean. *Geophysical Research Letters*, **35**, n/a–n/a.

Mohod, S.W. & Aware, M.V. (2012) Micro Wind Power Generator with Battery Energy Storage for Critical Load. *Ieee Systems Journal*, **6**, 118–125.

Molina, M.G., Suvire, G.O. & Mercado, P.E. (2012) Compensation of Wind Generator Power Fluctuations in Microgrid Applications by Superconducting Magnetic Energy Storage. *International Review of Electrical Engineering-Iree*, **7**, 3957–3968.

National Ambient Air Quality Standards (NAAQS) | Air and Radiation | US EPA. (2012) URL http://www.epa.gov/air/criteria.html [accessed 15 April 2013]

Climate Data Online: Text & Map Search. (2009) Governmental. URL http://www.ncdc.noaa.gov/cdo-web/

Nelson, P.F., Tibbett, A.R. & Day, S.J. (2008) Effects of vehicle type and fuel quality on real world toxic emissions from diesel vehicles. *Atmospheric Environment*, **42**, 5291–5303.

Niknam, T., Golestaneh, F. & Malekpour, A. (2012) Probabilistic energy and operation management of a microgrid containing wind/photovoltaic/fuel cell generation and energy storage devices based on point estimate method and self-adaptive gravitational search algorithm. *Energy*, **43**, 427–437.

Prasai, A., Paquette, A., Du, Y., Harley, R. & Divan, D. (2010) Minimizing emissions in microgrids while meeting reliability and power quality objectives. *Power Electronics Conference (IPEC), 2010 International* pp. 726 –733.

Prodromidis, G.N. & Coutelieris, F.A. (2012) Simulations of economical and technical feasibility of battery and flywheel hybrid energy storage systems in autonomous projects. *Renewable Energy*, **39**, 149–153.

Sydbom, A., Blomberg, A., Parnia, S., Stenfors, N., Sandström, T. & Dahlén, S.-E. (2001) Health effects of diesel exhaust emissions. *European Respiratory Journal*, **17**, 733–746.

Tauseef, S.M., Rashtchian, D. & Abbasi, S.A. (2011) CFD-based simulation of dense gas dispersion in presence of obstacles. *Journal of Loss Prevention in the Process Industries*, **24**, 371–376.

Tomas, R.A. & Webster, P.J. (1997) The role of inertial instability in determining the location and strength of near-equatorial convection. *Quarterly Journal of the Royal Meteorological Society*, **123**, 1445–1482.

Underwood, C.P., Ramachandran, J., Giddings, R.D. & Alwan, Z. (2007) Renewable-energy clusters for remote communities. *Applied Energy*, **84**, 579–598.

Wijayatunga, P.D.C., Fernando, W. & Shrestha, R.M. (2004) Impact of distributed and independent power generation on greenhouse gas emissions: Sri Lanka. *Energy Conversion and Management*, **45**, 3193–3206.

Wu, S.-S., Qiu, X. & Wang, L. (2005) Population Estimation Methods in GIS and Remote Sensing: A Review. *GIScience and Remote Sensing*, **42**, 80–96.

Yang, K. & Walid, A. (2013) Outage-Storage Tradeoff in Frequency Regulation for Smart Grid With Renewables. *IEEE Transactions on Smart Grid*, **4**, 245–252.

APPENDIX A: Annual Wind Velocity Variation

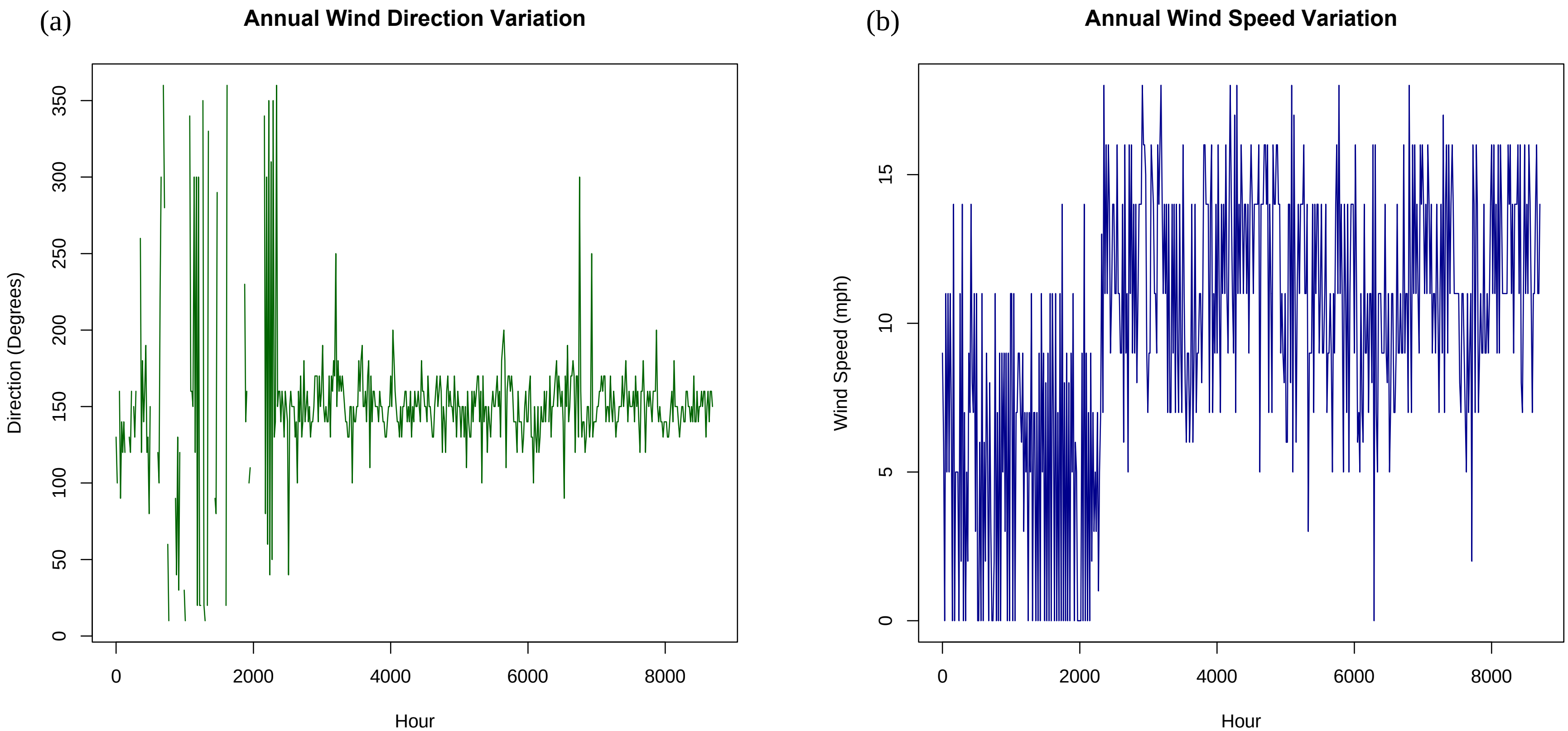

Fig. 6: Annual wind dataset for Puerto Villamil. (a) Variation of wind direction throughout the course of the year. Although there is appreciable variation seen in the late winter months, the remainder of the year sees very little variation, and a predominant wind direction focused around 160 degrees. This invariability was a major driver of the exposure values noted in each of the models. (b) Annual wind speed variation. Though there is much greater variation in wind speed, the graph demonstrates the non-zero tendency of the data. This non-static tenancy, in conjunction with the invariable directionality of the wind resulted in the patterns noted in the modeled exposure data.

APPENDIX B: Electricity Grid Parameters

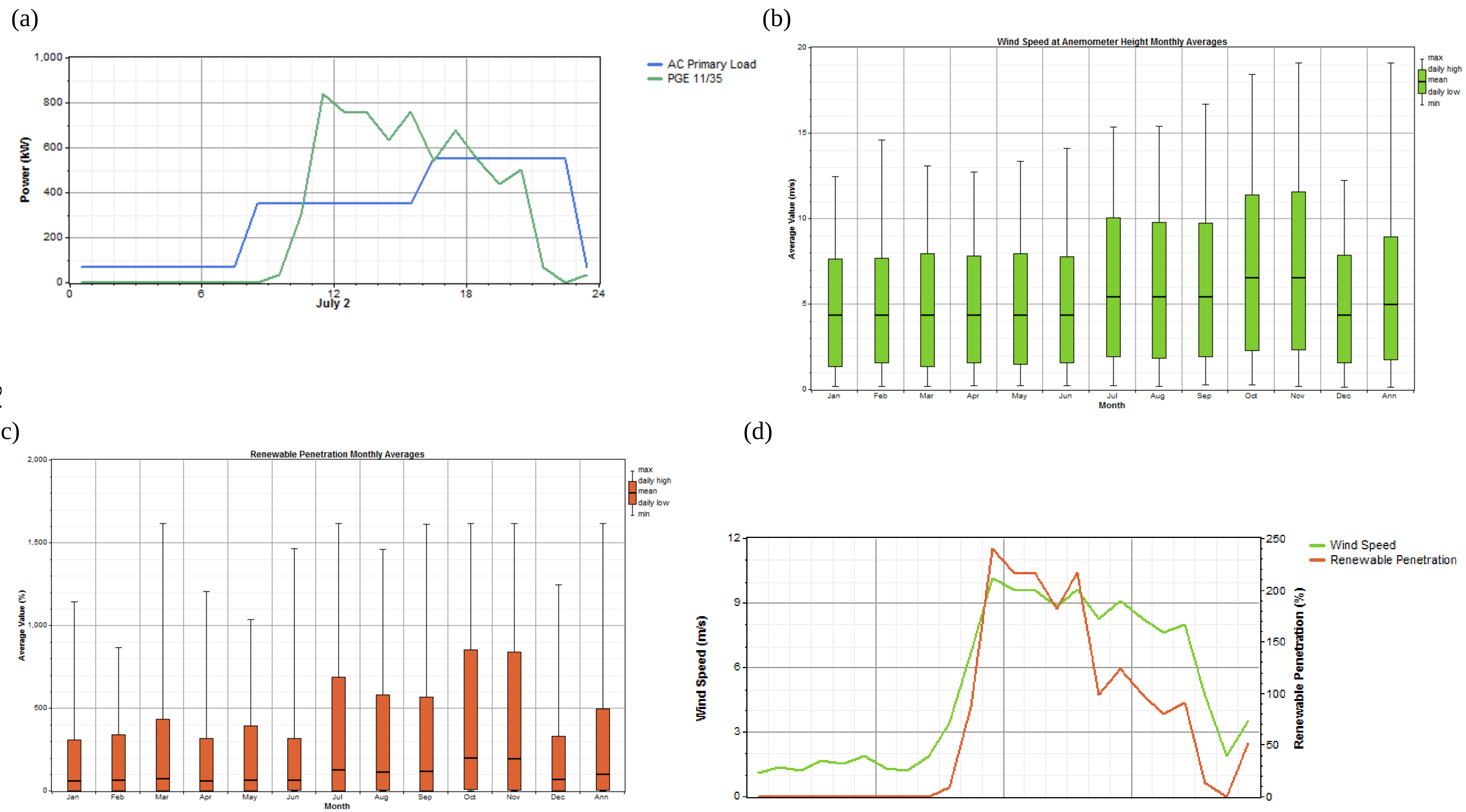

Fig. 7. Electricity grid parameters modeled in HOMER. (a) A load profile for Puerto Villamil shown in blue, indicative of the average power consumption tendencies for grid-connected loads. Power output from the wind turbines shown in green. The peaks for load and renewable supply are not temporally coincident, mandating the inclusion of battery storage. (b) Graphical representation of wind speed throughout the year. (c) Renewable penetration throughout the year. (b) A composite of the two previous parameters indicating the direct relationship between the wind availability and renewable penetration.

APPENDIX C: Prevailing Wind Patterns of Equatorial Latitudes

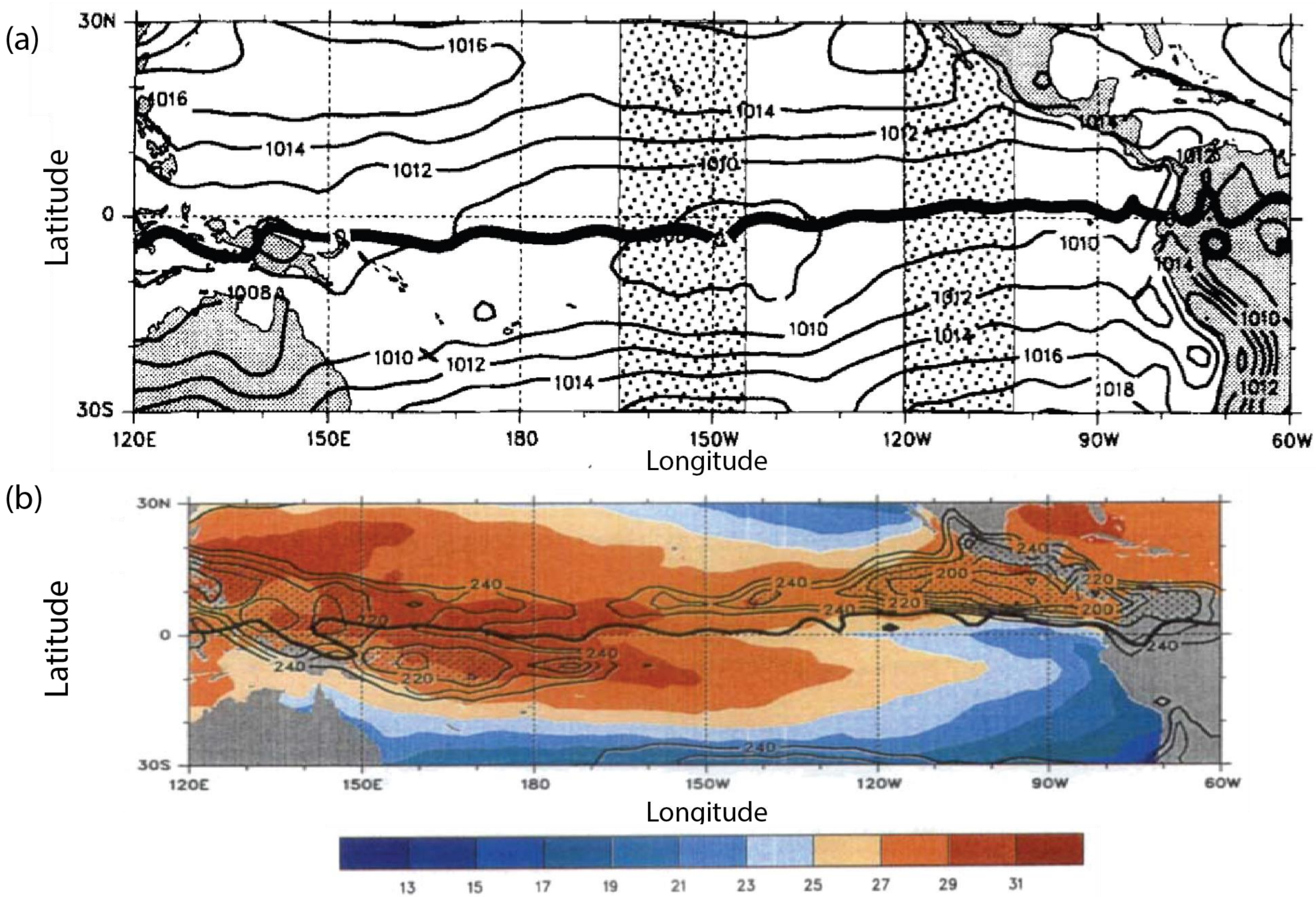

Fig. 8. Meteorological conditions near the equator. (a) Distributions of sea-level pressure (SLP) between 30N and 30S. Bold line denotes zero vorticity, a term used to describe the rotation of a fluid, in this case induced by the spinning of the earth. Puerto Villamil, slightly below the equator and at 90˚W, is proximal to this 0 vorticity point and is thereby more subject to outgoing long wave radiation to dictate directionality of prevailing winds (Tomas and Webster 1997). (b) Geospatial information system displaying a distribution of outgoing long-wave radiation (OLR) in Wm^{-2} from the ocean. The region near Puerto Villamil is relatively neutral in the spectrum. (Graphics from Tomas and Webster 1997.)